LARGE EDDY SIMULATIONS OF TURBULENT FLOWS AT SUPERCRITICAL PRESSURE

C. Kunik¹, I. Otic¹ and T. Schulenberg¹

¹ Karlsruhe Institute of Technology (KIT), Karlsruhe, Germany <u>claus.kunik@kit.edu</u>, <u>ivan.otic@kit.edu</u>, <u>thomas.schulenberg@kit.edu</u>

Abstract

A Large Eddy Simulation (LES) method is used to investigate turbulent heat transfer to CO_2 at supercritical pressure for upward flows. At those pressure conditions the fluid undergoes strong variations of fluid properties in a certain temperature range, which can lead to a deterioration of heat transfer (DHT).

In this analysis, the LES method is applied on turbulent forced convection conditions to investigate the influence of several subgrid scale models (SGS-model). At first, only velocity profiles of the so-called inflow generator are considered, whereas in the second part temperature profiles of the heated section are investigated in detail. The results are statistically analyzed and compared with DNS data from the literature [1].

Introduction

For the long term development of nuclear power, six novel reactor concepts of generation IV are proposed by the American Department of Energy (DOE) and the Generation IV International Forum (GIF, see [23]) to meet the future energy demand. One of these concepts is the supercritical water reactor (SCWR), which is cooled and moderated with water at supercritical pressure, e.g. [16], [23]. Main feature of this type of reactor is the increase of efficiency up to 45%. The reduction of size of several components is another advantage, which can lead to a reduction of costs. To give a better understanding on heat transfer for this type of reactor, fundamental numerical investigations are required.

At supercritical pressure conditions, the fluid always remains as a single phase, independent of its temperature. Close to the pseudo critical point, the thermophysical fluid properties vary very strongly with both, pressure and temperature. These nonlinear property changes have a significant influence on the heat transfer characteristic due to the interaction with the turbulence. Hence, the prediction of heat transfer at supercritical pressure conditions is very difficult and common heat transfer correlations (e.g. Dittus-Boelter) are not valid. Fig. 1 shows the changes for specific heat capacity and thermal conductivity at several pressures for CO₂. The thermodynamic critical point of this fluid is at the temperature of 304.15 K and the pressure of 7.37 MPa. The figure illustrates the decreasing gradients of fluid property changes with increasing pressure.

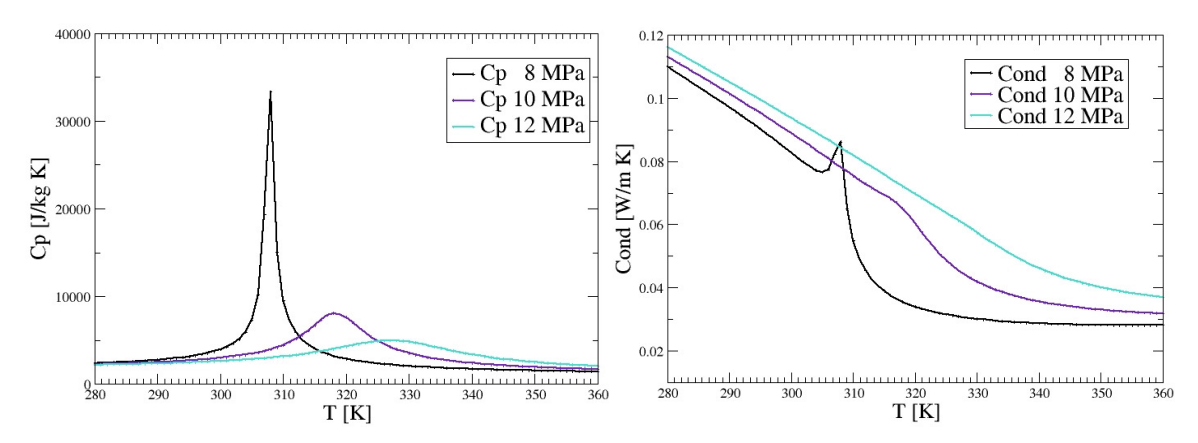


Figure 1 Thermophysical properties of CO2 at various pressure conditions.

There are two challenges concerning the heat transfer at supercritical pressure. The first one is the enhancement of heat transfer, which is mainly detected for upward directed pipe flow, e.g., [10]. This phenomenon occurs at high mass fluxes and low heat fluxes. For nuclear application, the enhancement of heat transfer is preferable, due to the increasing efficiency of the reactor. The second phenomenon is the more challenging one for safety analysis of the reactor. The so-called deterioration or impairment of heat transfer (DHT) occurs at low mass fluxes and high heat fluxes, e.g. [10], [11]. The high heat up in the near wall area and the associated property changes, in conjunction with the dominating buoyancy effect, leads to a decreased production of turbulent kinetic energy. This so-called relaminarisation effect, especially for upward directed flows, is one of the reasons for the impairment of heat transfer, which can lead to material damages for the fuel cladding. Due to the fact that the full mechanism, which leads to this phenomenon, is still not completely understood, many research facilities and universities are doing experimental and numerical investigations, see e.g. [12], [13], [15]. Surveys of experimental investigations of heat transfer in supercritical water and CO2 up to the year 2005 are given in e.g. [4] and [18]. A more general overview of the heat transfer phenomena and actual heat transfer correlations are given in [7], [19].

Experimental studies are quite expensive and cannot provide data concerning the flow and temperature field in the near wall area. To investigate the effects which are responsible for the DHT phenomena, some direct numerical simulations (DNS) have been performed for very simple geometries, e.g. [1], [2]. The DNS analysis can replace experimental investigations, but is restricted to low Reynolds numbers because of the computational effort. Therefore several authors suggest the Reynolds Averaged Navier Stokes (RANS) method, which is much faster e.g. [3], [9], [24]. Many approaches have been made to adapt the turbulence models used in the RANS method to catch the effects of heat transfer at supercritical pressure, but up to now, there is no common model which can give the DHT phenomenon or the enhancement of heat transfer [7], [8]. To overcome the disadvantage of computational effort of a DNS and the time averaging of a RANS method, a Large Eddy Simulation (LES) can provide detailed data of the flow and temperature field.

In this work a LES-method, in which all thermophysical properties are dependent on temperature at a constant pressure, is implemented in the open source software OpenFOAM.

This approach accounts for the strong fluid property variations. In the first part, the flow field of the so-called inflow generator is investigated using several subgrid scale (SGS) models to prove the capability and the mesh dependency of each model. The results are validated with DNS data according to [1] and [5]. In the second part, heat transfer at forced convection condition is investigated. The results show a strong dependency on the used SGS model for flow and temperature field.

1. Governing equation

In this LES-approach, the compressible Navier Stokes equations are used to account for the strong variations of fluid properties. All thermodynamic state variables, like density ρ or dynamic viscosity μ are determined dependent on temperature at a constant pressure p_0 in all terms of the conservation equations. The acoustic interaction at high Mach numbers is neglected due to the application of this method on low Reynolds numbers. With these assumptions and the standard Leonard decomposition $\psi = \tilde{\psi} + \psi'$ for any variable $\psi = u_i, p, h, ...$, where $\tilde{\psi}$ is the resolved part and ψ' is the modelled part, the compressible conservation equations are given as:

Continuity equation:

$$\frac{\partial \tilde{\rho}}{\partial t} + \frac{\partial \left(\tilde{\rho u_i}\right)}{\partial x_i} = 0 \tag{1}$$

Momentum equation:

$$\frac{\partial \left(\rho \tilde{u}_{i}\right)}{\partial t} + \frac{\partial \left(\rho \tilde{u}_{i} \tilde{u}_{j}\right)}{\partial x_{i}} = -\frac{\partial \tilde{p}}{\partial x_{i}} + \frac{\partial}{\partial x_{i}} \left[2\mu_{eff} \tilde{S}_{ij} - \frac{2}{3}\mu_{eff} \tilde{S}_{ii} \delta_{ij}\right]$$

$$(2)$$

Energy equation:

$$\frac{\partial \left(\rho \tilde{h}\right)}{\partial t} + \frac{\partial \left(\rho u_{j} \tilde{h}\right)}{\partial x_{j}} = \frac{\partial}{\partial x_{j}} \left(a_{eff} \frac{\partial \tilde{h}}{\partial x_{j}}\right) \tag{3}$$

where

$$\tilde{S}_{ij} = \frac{1}{2} \left(\frac{\partial \tilde{u}_i}{\partial x_j} + \frac{\partial \tilde{u}_j}{\partial x_i} \right) \tag{4}$$

denotes the strain rate tensor and δ_{ij} the Kronecker delta. The energy equation is given in the enthalpy form wherein the effective thermal conductivity α_{eff} is defined as

$$\alpha_{eff} = \alpha + \alpha_{SGS} \tag{5}$$

where α_{SGS} is the modelled SGS thermal conductivity added to the thermal conductivity. The SGS part is coupled with the SGS eddy viscosity μ_{SGS} and modelled with help of the turbulent Prandtl number Pr_r . Usually the system of equations (1) - (3) is closed with the ideal gas equations, but this equation is not valid for supercritical pressure conditions. Instead the NIST data tables are used to determine the density.

Several SGS-models are used to determine the sub-grid scale eddy viscosity. The first model is a zero-equation model, also known as the Smagorinsky model, see [21], where μ_{SGS} is determined as follows,

$$\mu_{SGS_{ij}} = \left(C_{\varepsilon}l\right)^{2} \left[\frac{1}{2} \left(\frac{\partial \tilde{u}_{i}}{\partial x_{j}} + \frac{\partial \tilde{u}_{j}}{\partial x_{i}} \right)^{2} \right]^{1/2}$$
 (6)

where C_s is a constant and set to be 1.05. The character l denotes a characteristic length scale, e.g. the mean grid width Δ . It is commonly known, that this model could have same problems in free shear layers, reattaching flows and flows with large scale unsteadiness like wall dominated flows, e.g. in channels and pipes. To overcome these deficiencies, a one equation model is also applied, where the SGS-eddy viscosity will be determined from an additional transport equation for turbulent kinetic energy k:

$$\underbrace{\frac{\partial(\rho k)}{\partial t}}_{time} + \underbrace{\nabla^*(\rho \tilde{u} k)}_{convection} - \underbrace{\nabla^*[(\mu + \mu_{SGS})\nabla k]}_{diffusion} = \underbrace{\left(2\mu_{SGS}\tilde{S}_{ij} - \frac{2}{3}\rho k\delta_{ij}\right)}_{production} \tilde{S}_{ij} - \underbrace{\frac{C_{\varepsilon}\rho k^{3/2}}{\Delta}}_{production} \tag{7}$$

 $\rho C_{\varepsilon} k^{3/2} / \Delta = \varepsilon$ is the turbulent dissipation at the smallest scales. The SGS-eddy viscosity is calculated as follows

$$\mu_{SGS} = \rho C_k k^{1/2} \Delta \tag{8}$$

The coefficient C_k is set to be 0.07 and C_{ε} is set to be 1.05. A disadvantage of this model is the additional transport equation, which leads to an increasing of the computational effort. In case of relaminarisation or energy back scattering both models are also not the preferable ones. Therefore a third model, the so called dynamic one equation model, has been considered. Here, the coefficient C_k of Eq. 8 is determined as a variable in space. Details to this kind of SGS modelling can be found in [6] and Lilly et al. [14]. The equations are solved using the PISO-algorithm for transient simulations with second order differencing schemes in time and space. The results are given in dimensionless form using

$$y^{+} = \frac{y u_{\tau}}{V}, \quad u_{\tau} = \sqrt{\frac{\tau_{w}}{\rho}}, \quad u^{+} = \frac{u}{u_{\tau}}, \quad T_{w}^{+} = \frac{T_{w}}{T_{0}}$$
 (9)

where y^+ is the dimensionless wall distance, u_{τ} the friction velocity, τ_w the wall shear stress, T_w the wall temperature and T_0 a constant reference temperature. The initial Reynolds number is given by

$$Re_{0} = \frac{u_{0} L \rho_{0}}{\mu_{0}} \tag{10}$$

where L is a characteristic length scale. The velocity fluctuations are defined as

$$u_{rms} = \sqrt{\overline{u'^2}} \tag{11}$$

2. Application of LES-method - Computational domain

A direct numerical simulation [1] of upward directed turbulent pipe flow in CO_2 at supercritical pressure conditions is chosen to validate the code. Fig. 2(a) shows the geometry of the DNS, including an inflow generator and a heated section. The diameter D is 1 mm.

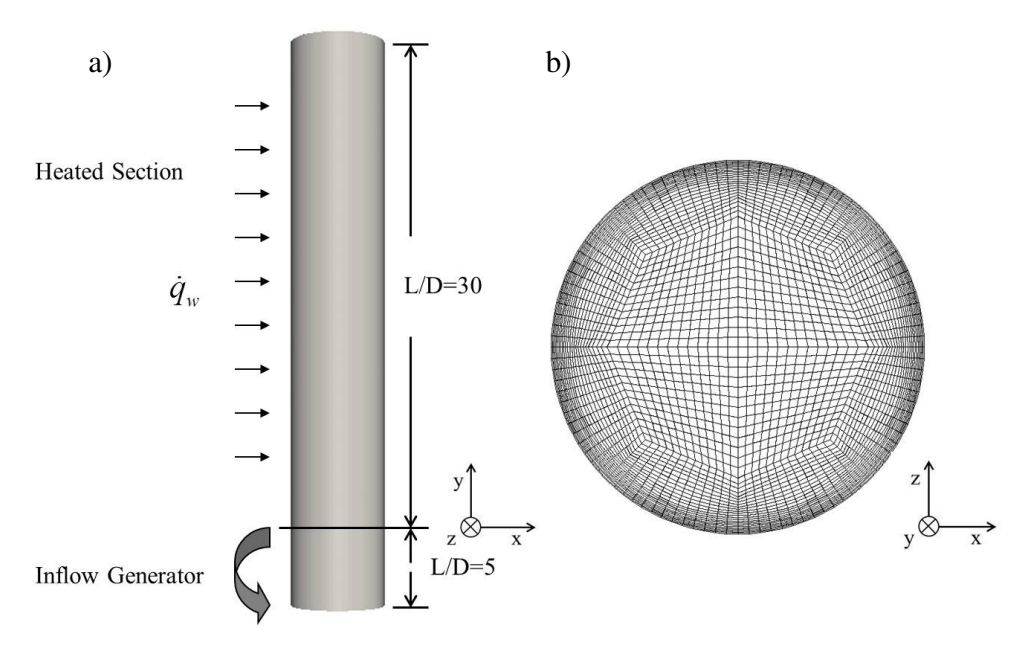


Figure 2 (a) Computational domain; (b) Mesh (Top View).

The length to diameter distribution (L/D=5) is chosen to obtain a fully developed flow field inside of the inflow generator. Therefore cyclic boundary conditions at isothermal conditions are applied to derive velocity and turbulent kinetic energy profiles. The pressure is 8 MPa, where the associated pseudocritical temperature is at 307.85 K, so the inlet temperature is chosen to be 301.15 K. This pressure is applied as a constant to the outlet of the heated section. In the literature [1], the Reynolds number is given with a value of 5400. Using NIST data tables, the bulk velocity is determined as $u_0 = 0.4454 \, m/s$. This value is given as initial

condition to the internal field which is afterwards perturbed to accelerate the development of a fully developed flow field. The initial value for turbulent kinetic energy is set to be zero at the wall and the internal field. Furthermore, no-slip boundary conditions are applied to the wall with a constant heat flux of $\dot{q} = 61.74 W/m^2$ for the heated section to cover the pseudocritical region. Advective boundary conditions are used for the temperature field at the outlet. For μ_{SGS} and α_{SGS} zero gradient boundary conditions are applied to the wall and the outlet. The mesh, shown in Fig. 2 b) is based on an octagon with a refinement to the wall.

3. Results

Fig. 3 shows the dimensionless velocity profiles of the inflow generator, using the Smagorinsky SGS-model (a), the one equation model (OE, b) and the dynamic one equation model (c). The results are compared with DNS data from Bae et al. (black) [1], Eggels et al. (light blue) [5] and the logarithmic wall law. In the first analysis, the simulations are performed with a relatively course mesh, which consists of 103400 cells ($y^+ \approx 0.5$). This corresponds to a mesh resolution of about 29 cells in radial direction and 50 cells in streamwise direction.

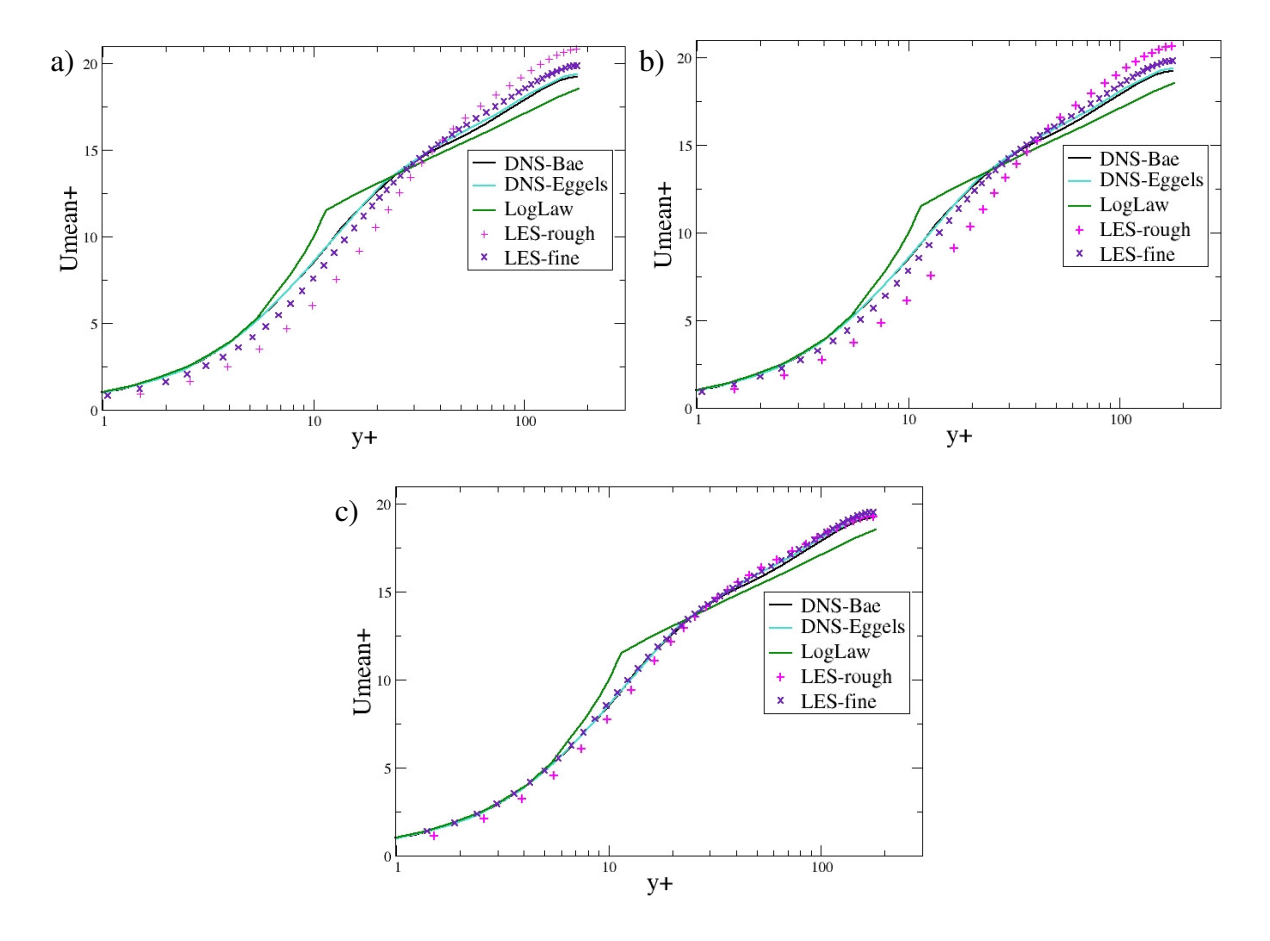


Figure 3 Mean velocity distribution for (a) Smagorinsky, (b) OE and (c) dynamic OE model.

The results are shown in magenta (+), whereas the results of the analysis using a finer mesh resolution (633000 cells, 53 radial, 100 axial, $y^+ \approx 0.25$) are given in violet (x). It is shown that, for all SGS-models used in the present calculations, the results are getting better with increasing mesh size. However, the calculations using the dynamic OE model show much better results for both mesh resolutions, than the Smagorinsky or standard OE model.

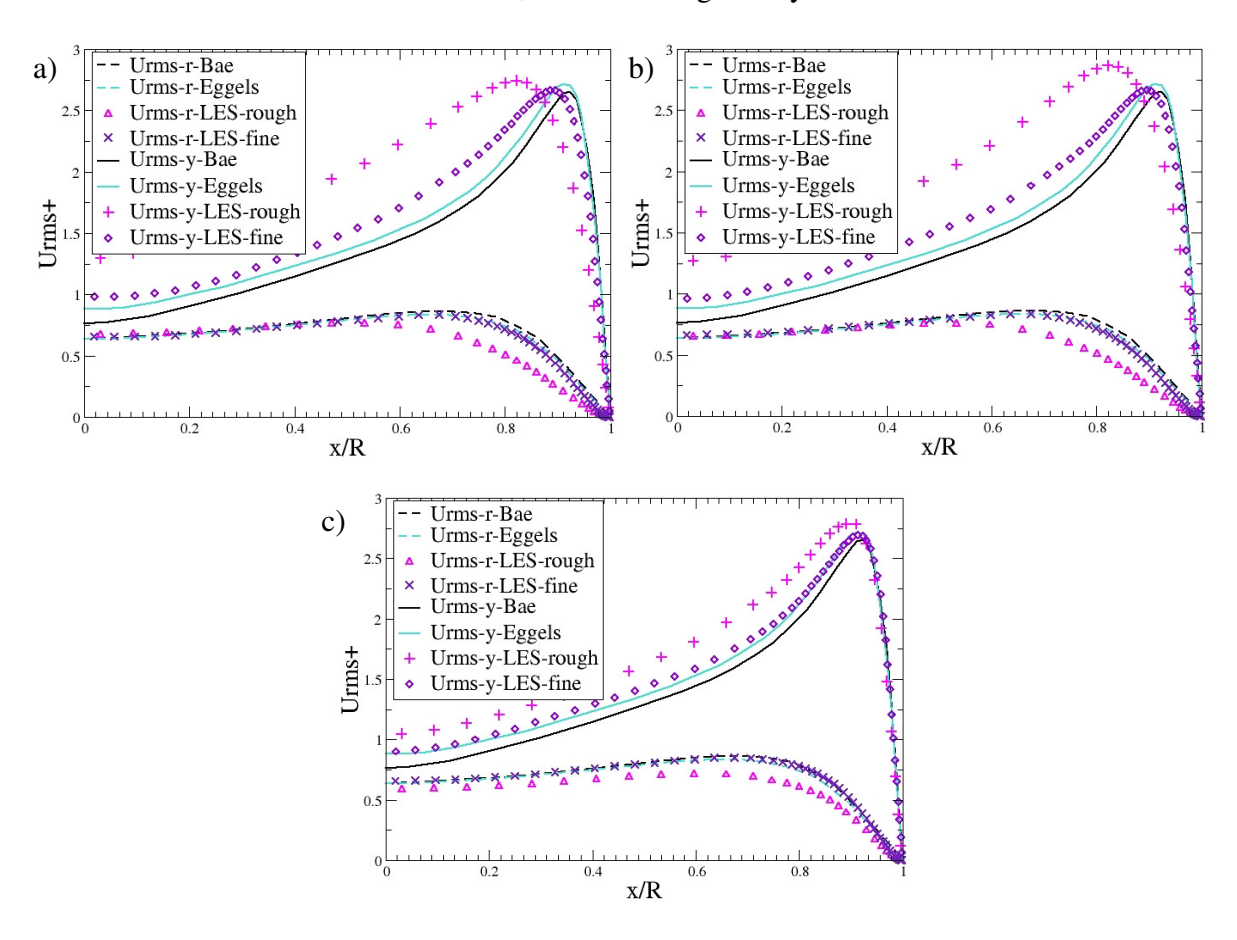


Figure 4 Velocity fluctuation profiles for Smagorinsky (a), OE (b) and dynamic OE model (c).

The same conclusion is valid for the turbulent kinetic energy (TKE) profiles, especially for the root mean squared (rms) values in radial (Urms-r) and streamwise (Urms-y) direction, which are plotted over the dimensionless radius, see Fig. 4, where x is the radial coordinate and R the fixed radius of the pipe. In the upper left the results, using the Smagorinsky model, are shown. The dashed black line denotes the results of the DNS of Bae et al. in radial direction, the dashed light blue line the results of the DNS of Eggels et al., the triangles the results of the LES-method using a courser grid and the cross the results using the finer mesh. The results of the rms-values in streamwise direction are given in straight lines for the DNS, whereas the results of the LES method are given in plus (+) for the course mesh and in diamonds for the finer mesh. It is shown that there is a difference in the results of the DNS of Bae and Eggels, which is in particular remarkable for the streamwise direction. The results of LES method

using the Smagorinsky model (a) and the OE model (b) are quite similar. There is a big improvement of the results using a finer mesh. However, the results using the dynamic OE (c) model are much better for both meshes.

The second investigation considers the heated section. The mesh resolution used for this analysis is about 723000 cells, which is equivalent to the courser mesh used for the inflow generator. y^+ is about 0.5. This is sufficient, because the main influence on the results is not the mesh resolution as will be shown later. Furthermore, the results of the LES method using the dynamic OE model are quite good for the mean velocity field, see Fig 5. The straight lines denote the DNS results at the inlet (y = 0 mm), at y = 5 mm, at y = 15 mm and the outlet (y = 30 mm), whereas the squares show the results for the LES method at the same axial heights. The turbulent Prandtl number, used for this analysis is chosen to be 0.5. There is a very good agreement between LES and DNS data. The LES method reproduces the influence of thermally induced flow acceleration much better than a RANS method, e.g. [9]. In that case, the acceleration effect in the heated section is strongly overestimated along the axial length.

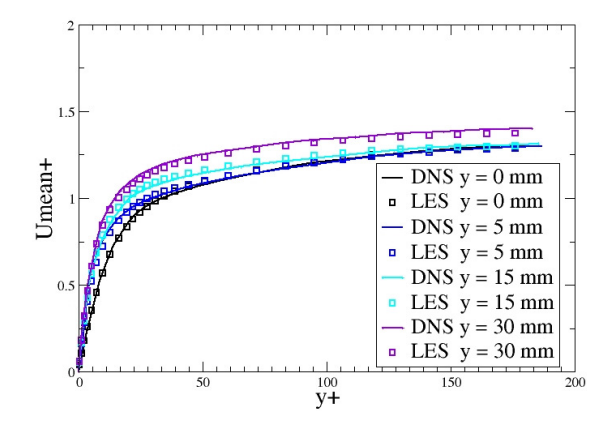
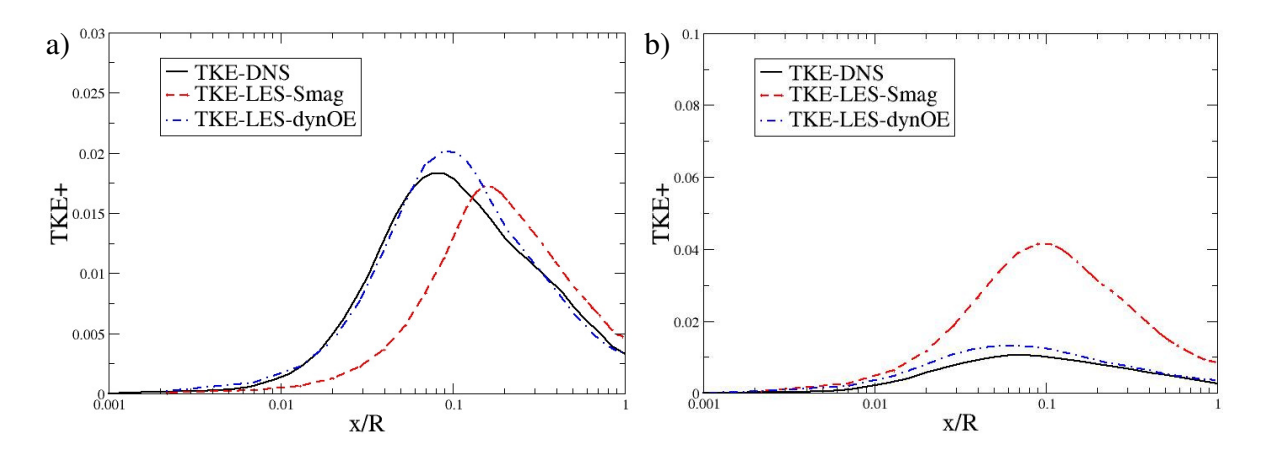


Figure 5 Velocity profiles along the heated length.

Fig. 6 shows the associated characteristics of the turbulent kinetic energy (TKE). Here, the dimensionless turbulent kinetic energy is plotted logarithmically over the dimensionless radius.



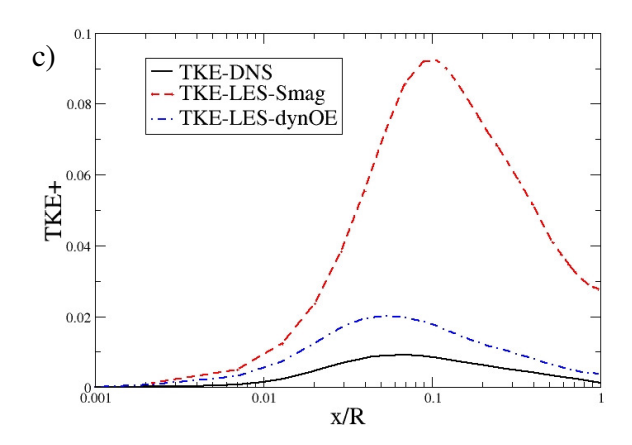


Figure 7 TKE energy profiles over the heated length (a) y = 0 mm, (b) y = 15 mm, (c) y = 30 mm.

Again, the straight black line denotes the DNS data, the dashed red line the LES method using the Smagorinsky model and the dashed dotted blue line represents the LES data using the dynamic OE model. The results of the OE model are similar to the Smagorinsky model and therefore not shown. Attention should be paid on the different scales used for the y axis of Fig. 6(a) and Fig. 6(b), 6(c). There is a good agreement between the results of the LES method using the dynamic OE model and the DNS data at the inlet (Fig. 6(a)) and the middle of the heated section (Fig 6(b)), but at the outlet the TKE is overestimated. The deviations of the LES method using the Smagorinsky model are much higher along the heated section. This behaviour is due to the interaction of the turbulence with the nonlinear thermal property changes in the near wall area. The SGS models are not able to capture these effects. As a consequence, the LES method is not able to give good results of the wall temperature distribution.

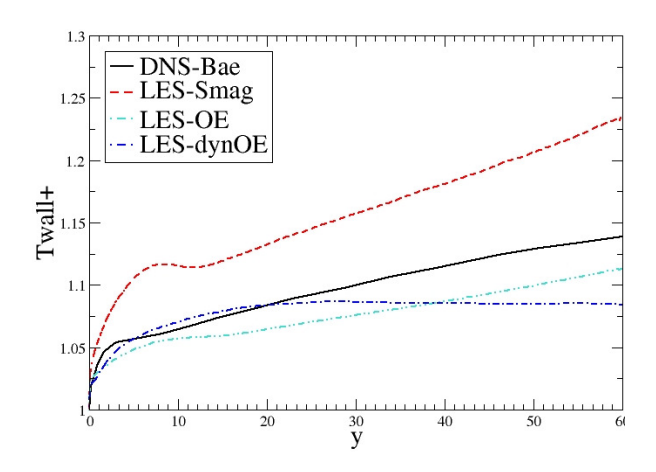


Figure 7 Wall temperature distribution.

Fig. 7 shows the distribution of the wall temperature over the heated length, where the given data from the literature are denoted by the black line, the results of the LES method using the Smagorinsky model by the dashed red line, the results using the OE model by the dashed

double dotted light blue line and the results using the dynamic OE by the dashed dotted blue line. The Smagorinsky model overestimates the wall temperature in contrast to the other SGS models. Hence, every SGS model shows a different behaviour in the near wall area, where production of turbulence is influenced by the fluid property changes. There, the applied constant turbulent Prandtl number cannot take into account the nonlinear coupling of the velocity and the enthalpy, which leads to big inconstancies. This is the main reason for the differing results. The mesh resolution plays a subordinate role. There is also a discrepancy in the bulk temperature distribution, see Fig. 8.

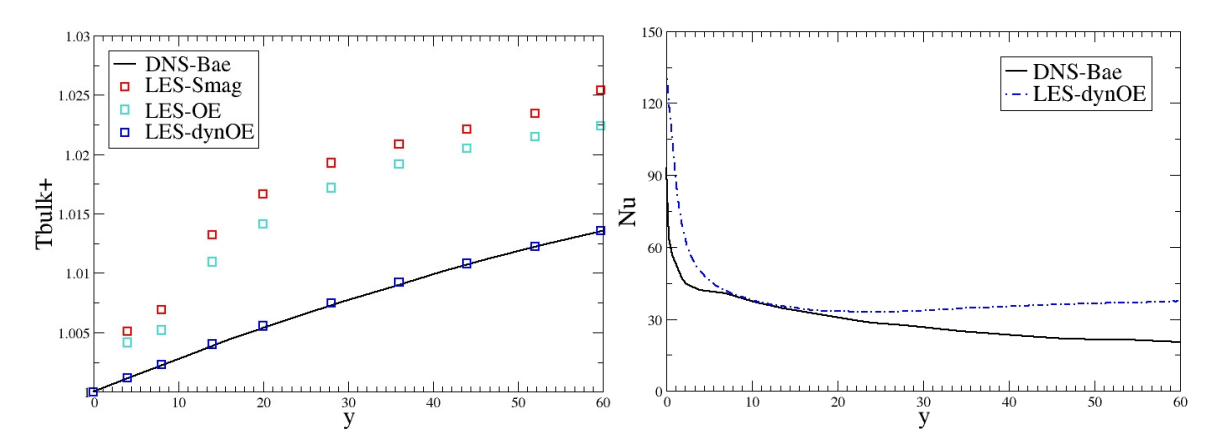


Figure 8 Bulk temperature and Nusselt number distribution over the heated length.

The definition of the dimensionless bulk temperature is given as

$$\dot{m} = \int_{A} \overline{\rho \left| u_{y} \right|} dA, \quad h_{b} = \frac{1}{\dot{m}} \int_{A} \overline{\rho \left| u_{y} \right|} h dA, \quad T_{b}^{+} = \frac{T_{b} \left(p_{0}, h_{b} \right)}{T_{0}}$$
(3)

where \dot{m} denotes the mass flow rate and h_b the bulk enthalpy. The corresponding bulk temperature is calculated with help of the NIST data tables. Both models, the Smagorinsky and the OE model (red and light blue squares) overestimate the bulk temperature, whereas the results of the dynamic OE model (blue squares) are in very good agreement with the given data. Because of the dependency of the Nusselt number on the wall and bulk temperature, only the Nusselt number profile for the dynamic OE model is plotted. The definition is given as

$$Nu = \frac{\alpha D}{\lambda_b}, \quad \text{with} \quad \alpha = \frac{\dot{q}_w}{T_w - T_b}$$
 (14)

The overestimation is due to the underestimation of the wall temperature especially at the outlet.

4. Conclusion

A large eddy simulation method is applied on turbulent forced convection at supercritical pressure. It is shown, that an sufficiently fine mesh resolution gives good results for all used SGS-models for the inflow generator. However, for courser mesh resolution the dynamic OE

model is preferable. This proposition is also valid for the second application, including the heated section. The velocity distribution and bulk temperature distribution are in very good agreement with given DNS data. Only TKE profiles in the upper part of the heated section show a deviation which results into a lower wall temperature. In contrary to those results, the Smagorinsky model and the standard one equation model are not suitable for heated turbulent flows at supercritical pressure. To overcome the disadvantage of the dynamic OE model, a DNS method is suggested for the near wall area. This will take into account the effects of nonlinear property changes to the production of TKE. In the bulk, the LES method using the dynamic OE model is suggested. This DNS/LES method will be applied also on mixed convection conditions and promises best results at supercritical pressure conditions.

5. References

- [1] J. H. Bae, J. Y. Yoo, H. Choi, "Direct numerical simulation of turbulent supercritical flows with heat transfer," *Physics of Fluids*, **17**, pp. 105104-01-105104-24 (2005).
- [2] J. H. Bae, J. Y. Yoo, D. M. McEligot, "Direct numerical simulation of heated CO₂ flows at supercritical pressure in a vertical annulus at Re = 8900," *Physics of Fluids*, 20, pp. 055108-01-055108-20 (2008).
- [3] X. Cheng, B. Kang, Y. H. Yang, "Numerical analysis of heat transfer in supercritical water cooled flow channels," *Nuclear Engineering and Design*, **237**, pp. 240-252 (2007).
- [4] R. B. Duffey, I. L. Pioro, "Experimental heat transfer of supercritical carbon dioxide flowing inside tubes (survey)," *Nuclear Engineering and Design*, **235**, pp. 913-924 (2005).
- [5] J. G. M. Eggels, F. Unger, M. H. Weiss, J. Westerweel, R. J. Adrian, J. Friedrich, F. T. M. Nieuwstadt, "Fully developed turbulent pipe flow: a comparison between direct numerical simulation and experiment," *J. Fluid Mech.*, **268**, pp. 175-209 (2005).
- [6] M. Germano, U. Piomelli, P. Moin, W. Cabot, "A dynamic subgrid-scale eddy viscosity model," *Phys. Of Fluids*, **3**, no. 7, pp. 1760-1765 (1991).
- [7] S. He, W. S. Kim, P. X. Jiang, J. D. Jackson, "Simulation of mixed convection heat transfer to carbon dioxide at supercritical pressure," *J. Mech. Eng. Sci.*, **218**, pp.1281-1296 (2004).
- [8] S. He, W. S. Kim, J. D. Jackson, "A computational study of convective heat transfer to carbon dioxide at a pressure just above the critical value," *Applied Thermal Eng.*, **28**, pp. 1662-1675 (2008).
- [9] S. He, W. S. Kim, J. H. Bae, "Assessment of performance of turbulence models in predicting supercritical pressure heat transfer in a vertical tube," *Int. J. of Heat and Mass Transfer*, **51**, pp. 4659-4675 (2008).
- [10] J. D. Jackson, W. B. Hall, "Forced convection heat transfer to fluids at supercritical pressure," *Turbulent forced convection in channels and bundles*, **2**, pp.563-611 (1979).

- [11] J. D. Jackson, W. B. Hall, "Influences of buoyancy on heat transfer to fluids flowing in vertical tubes under turbulent conditions," *Turbulent forced convection in channels and bundles*, **2**, pp. 613-640 (1979).
- [12] H. Y. Kim, Y. Y. Bae, "Experimental study on heat transfer to supercritical CO2 in a circular tube," *16th Pacific Basin Nuclear Conference (16PBNC)*, Aomori, Japan, Oct. 13-18, PaperID P16P1025 (2008).
- [13] J. Licht, M. Anderson. M. Corradini, "Heat transfer and fluid flow characteristics in supercritical water," *Journal of Heat Transfer*, **131**, pp. 072502-1 072502-14 (2009).
- [14] D. K. Lilly, "A proposed modification of the Germano sub-grid scale closure method," *Phys. Fluids A*, 4, pp. 633-635 (1991).
- [15] T. Misawa, H. Yoshida, H. Tamai, K. Takase, "Numerical analysis of heat transfer test of supercritical water in a tube using the three dimensional two-fluid model code," *J. of Power and Energy Systems*, **3**, No. 1, pp.194-203 (2009).
- [16] Y. Oka, Y. Ishiwatari, S. Koshizuka, "Research and development of super LWR and super fast reactor,"Proceedings of the 3rd Int. Symposium on SCWR-Design and Technology, Shanghai, China, March 12-15, Paper no. I003 (2007).
- [17] I. L. Pioro, H. F. Khartabil, R. B. Duffey, "Heat transfer to supercritical fluids flowing in channels empirical correlations (survey)," *Nuclear Engineering and Design*, **230**, pp.69-91 (2004).
- [18] I. L. Pioro, R. B. Duffey, "Experimental heat transfer of supercritical water flowing inside channels (survey)," *Nuclear Engineering and Design*, **235**, pp. 2407-2430 (2005).
- [19] I. L. Pioro, H. F. Khartabil, R. B. Duffey, "Heat transfer at supercritical pressures (survey)," 11th International Conference on Nuclear Engineering, ICONE11-36454, Tokio, Japan, April 20-23 (2003).
- [20] S. B. Pope, *Turbulent Flows*, Cambridge University Press, Cambridge (2003)
- [21] J. Smagorinsky, "General circulation experiments with the primitive equations, I, The basic experiment," *Mon. Weather Rev.*, **91**, pp. 99-164 (1963).
- [22] T. Schulenberg, J. Starflinger, J. Heineke, "Three pass core design proposal for a high performance light water reactor," *Proceedings of INES-2 International Conference on Innovative Nuclear Energy Systems*, Yokohama, Japan, Nov. 26-30 (2006); published in Nuclear Engineering (2007).
- [23] US DOE Nuclear Energy Research Advisory Commitee, "A Technology Roadmap for Generation IV Nuclear Energy Systems," *Tech. Report*, Generation IV International Forum (2002).
- [24] Y. Zhu, E. Laurien, "Prediction of heat transfer of upward flow in annular channel at supercritical pressure water and CO2," 3rd International Symposium on Supercritical Water-Cooled Reactors, Heidelberg, Germany, March 8-11, Paper no. 35 (2009).